www.dergipark.gov.tr
ISSN:2148-3736
El-Cezerî Fen ve Mühendislik Dergisi
Cilt: 7, No: 3, 2020 (1201-1219)

El-Cezerî Journal of Science and Engineering
Vol: 7, No: 3, 2020 (1201-1219)
DOI :10.31202/ecjse.733519

ECJSE

Research Paper / Makale

A Novel Gray Image Enhancement Using the Regional Similarity Transformation Function and Dragonfly Algorithm

Ferzan KATIRCIOĞLU[1a], Zafer CINGIZ[2b]

University of Duzce, DMYO, Department of Electronics and Automation, Duzce, Turkey
University of Duzce, DMYO, Department of Energy, Duzce, Turkey
ferzankatircioglu@duzce.edu.tr

Received/Geliş: 07.05.2020 **Accepted/Kabul:** 17.08.2020

Abstract: Image enhancement is a necessary and indispensable technique for increasing the quality of digital images. The main task is to generate a new intensity value for each pixel in the image using a transformation function after the input image receives the intensity value of each pixel. The proposed transfer function in this study is called the Regional Similarity Transfer Function (RSTF) that considers the density distribution similarity between adjoining pixels. Dragonfly Algorithm (DA) intuitive optimization technique, which is preferred in engineering applications, has been used to optimize the parameter values of the proposed transfer function. Image quality evaluation is performed with six criteria between the improved and original images. Our experimental results show that the intensity distribution between adjoining pixels show an increase in contrast and brightness over the similarity degree. Excessive brightness, blur, and deterioration in the images is resolved with the proposed method.

Keywords: Gray Image Enhancement, Dragonfly Algorithm, Transformation Function.

Bölgesel Benzerlik Dönüşüm Fonksiyonu ve Yusufçuk Algoritması Kullanılarak Yeni Gri Görüntü İyileştirme

Öz: Görüntü iyileştirme, dijital görüntülerde görüntü kalitesini artırmak için gerekli ve vazgeçilmez bir tekniktir. Görüntü iyileştirme de temel görev, giriş görüntüsünün her bir pikselin yoğunluk değeri alındıktan sonra, dönüşüm fonksiyonu kullanarak, görüntü içerisinde karşılık gelen her piksel değeri için yeni bir yoğunluk değeri üretmektir. Çalışma da önerilen dönüşüm fonksiyonu Bölgesel Benzerlik Transfer Fonksiyonu olarak adlandırılmakta olup, komşu pikseller arasındaki yoğunluk dağılım benzerliğini dikkate alarak, dönüşüm uygulanmaktadır. Son zamanlarda mühendislik uygulamalarında çok tercih edilen Yusufçuk Algoritması sezgisel optimizasyon tekniği, önerilen dönüşüm fonksiyonunun parametre değerlerini optimize etmek amacıyla kullanılmıştır. Görüntü kalitesi değerlendirme işlemi, iyileştirilmiş ve orijinal görüntüler arasında altı kriterle gerçekleştirilmiştir. Deneysel sonuçlar, bitişik pikseller arasındaki yoğunluk dağılımının benzerlik derecesi üzerinde kontrast ve parlaklıkta bir artış gösterdiği tespit edilmiştir. Görüntülerdeki aşırı parlaklık, bulanıklık ve bozulma gibi istenmeyen durumlar, önerilen yöntemle çözülmektedir.

Anahtar Kelimeler: Gri Görüntü İyileştirme, Yusufçuk Algoritması, Transfer Fonksiyonu

1. Introduction

Image enhancement aims to reduce or remove deterioration in an image or to improve the image for a specific purpose using human observation or computer analysis methods [1]. Image enhancement techniques can be divided into transform domain and spatial domain categories. The transform

How to cite this article
Katırcıoğlu, F., Cingiz, Z., "*A Novel Gray Image Enhancement Using the Regional Similarity Transformation Function and Dragonfly Algorithm"*, El-Cezerî Journal of Science and Engineering, 2020, 7 (3); 1201-1219.

Bu makaleye atıf yapmak için
Katırcıoğlu, F., Cingiz, Z., *"Bölgesel Benzerlik Dönüşüm Fonksiyonu ve Yusufçuk Algoritması kullanılarak Yeni Gri Görüntü İyileştirme"*, El-Cezerî Fen ve Mühendislik Dergisi 2020, 7 (3); 1201-1219.
ORCID: a0000-0001-5463-3792, b0000-0003-3796-755X

domain contains running techniques in transforming the image frequency, while the spatial domain technique improvement the image pixels levels' contrast and brightness [2].

Methods used for adjustment of contrast and brightness enhance the details of the image so that is may be better understood and easily evaluated. Histogram Equalization (HE), a primary method used to adjust contrast and brightness, performs appropriate changes on pixel values of the input image and provides equalization against each pixel value of the output image [3]. Implementation of this method provides easy and fast results. However, it may also form unnatural brightness and low contrast for most images. Improved versions of HE has been proposed. For example, performing HE while maintaining the average brightness of the image was proposed as the bi-histogram equalization method [4]. In another study, obtaining useful and smooth images was accomplished by first performing aggregation and thresholding processes before HE [5]. Through a recursive mean-separate HE brightness protection feature, an effective enhancement for different image types was enabled for features such as reducing generic inconveniences in recursive sub-image HE [6,7]. The purpose of an equalization histogram method is to distribute histogram values evenly, and because these values are fixed, the desired improvement could not always be obtained.

Most researchers preferred a sigmoid function to improve the contrast and brightness of an image. Tanaka et al. used a generalized sigmoid, called the "multiple parametric sigmoid function," based on local area data by synthesizing each transformation from the study [8]. Kannan et al. recommended a modified sigmoid function based on mapping the curve to enhance sport images with poor lighting [9]. In another recent study, Verma et al. recommended another modified sigmoid function by using PSO. Parameterization was performed for low and high contrast images, and the most appropriate values were searched using an objective function based on edge and entropy of these parameters and PSO [10]. Because the desired agreement between the sigmoid function and input image was not obtained, contrast and brightness are not sufficient in the output images.

Heuristic optimization algorithms were applied resulting in effective image enhancement studies. Munteanu and Lazarescu applied a genetic algorithm (GA) to a subjective fitness function to perform contrast stretching on selected areas of an image. The operator, called the Gaussian uniform crossover, was used for each image with separate evaluation criteria based on the removal of the region. However, pixel intensity variety was low in the resulting output images [11]. In another study using GA, enhancement was achieved by increasing the number of edges of an image with an objective assessment criterion. An arrayed-bits was compounded upon the relation curve between the gray level of the input image and that of the output image [12]. However, an increased number of edges of the image does not constitute an improvement. In this study, while the number of edges increased, visual impurities were omitted. In 2000, Munteanu and Rosa used a conversion function that adjusts the contrast and brightness by calculating new pixel values by processing the adjoining pixels in the input image. Image improvement was performed by applying GA on a transformation function called the Local Transformation Function (LTF). An objective evaluation criterion was maintained by multiplying the sobel value, entropy value, and number of edges of the image [13]. Later, LTF was applied on the particle swarm optimization algorithm by Gorai and Ghosh in 2009, on Zhao Gravitational Search Algorithm in 2011, on Cuckoo Search Algorithm by Agrawal and Panda in 2012, on Differential improvement algorithm by Sarangi et al. in 2014, and on Grey-Wolf Optimizer algorithm by Murali and Jayabarathi in 2016 [14,15,16,17,18]. The output images from these approaches was not always satisfactory when evaluated visually. Excessive brightness occurred in some areas of the image resulting in some details of the image being lost. In 2014, Draa and Boaziz used an artificial bee colony algorithm, and explained that the LTF image conversion function caused distortions in the images and they compared results of the transformation function with a proposed gray level mapping method [19].

When image processing and image enhancement are applied according to the purpose to be used, it has many advantages such as speed, low cost and achieving the desired result. Thanks to the new techniques developed, today image processing and image enhancement play a facilitating role in many areas. In the study proposed by Demircioğlu, one of them, was created a model for a molar tooth in the computer environment, measuring the surface roughness of the original tooth and implant surface properties and processing the images obtained [20]. In another study proposed by Güvenoğlu et al., A system capable of real-time error detection on woven fabric was developed using image processing techniques. This system consists of a mechanism that provides real time woven fabric error control using the method of removing shear let conversion feature from image processing techniques on woven fabric images that are instantly recorded with a Full HD camera [21]. In the study proposed by Katırcıoğlu, it can be shown as an example of applying image processing and image enhancement studies to a different area. It has been suggested that the average temperature inside the greenhouse should be obtained with infrared images, air relative humidity with psychrometric graphics application and soil moisture values by multiple regression analysis method [22]. As an example of the change made in image enhancement techniques, Enginoğlu et all's suggested work. They proposed the Adaptive Cesáro Average Filter (ACmF) as a method of removing salt and pepper noises in their study for image enhancement purposes and they also presented some basic concepts on this subject [23]. Due to their application to wider areas, bionic algorithms have been included as a separate category in the field of image enhancement. In one of these studies, Katircioğlu et al. proposed a new image enhancement algorithm based on gravitational force and the lateral inhibition network [24].

This study proposes a transformation function based on the similarity of the distribution of intensity between adjoining pixels and the maximum grey level from the histogram curve. The maximum grey level value is labelled Max, and the contrast increases as pixels to the left approach a 0 value while pixels to the right approach a value of 255. In addition, contrast and brightness increase positively according to the degree of similarity of intensity distribution between adjoining pixels. As a result of this transformation function, excessive brightness, blur, and deterioration in the images are resolved. Moreover, natural and wide contrast enhancement are obtained. The parameters of the transformation function are optimized using the Dragonfly Algorithm (DA). Entropy value, number of edge pixels, and intensity of the pixels are used together as evaluation criteria enabling an objective evaluation. In the second part of the study, Local Transformation Function (LTF) is described along with the proposed Regional Similarity Transformation Function (RSTF), evaluation criteria, and DA optimization technique. Next, grey image enhancement using RSTF and the realization of the process are presented with a flowchart, and the results of this application are provided for comparison. The visual and numerical results obtained are examined followed by a final evaluation of the method with suggestions for future work.

2. Methods

2.1. Local Transformation Function

Image enhancement includes reducing or entirely removing deterioration on an image or to improve the image for a specific purpose [25]. The main task is to generate a new intensity value for each pixel using a transformation function on the input image, as defined by

$$g(i,j) = T[f(i,i)\,] \tag{1}$$

In Eq. (1), *f(i,j)* is the input image, *g(i,j)* is the output image, and *T* represents a transformation function applied to the pixel at *(i,j)*. Transformation functions that find the best values using

heuristic optimization techniques have been preferred as discussed above, such as LFT that adjusts the contrast and brightness by considering adjoining pixels from the input image [13].

$$g(i,j) = \frac{k * D}{\varphi(i,j) + b}[f(i,j) - c * m(i,j)] + m(i,j)^a \quad (2)$$

In Eq. (2), *m(i,j)* is the average value of the pixels in a specific local area and is calculated according to .

$$m(i,j) = \frac{1}{nxn}\sum_{x=0}^{n-1}\sum_{y=0}^{n-1} f(x,y) \quad (3)$$

Here, *nxn* refers to the local field with areas of 3 × 3 and 5 × 5 has been used in application.

$$K(i,j) = \frac{k * D}{\varphi(i,j) + b} \quad (4)$$

In Eq. (4), *K(i,j)* is an enhancement function and *D* is the global average value calculated for the entire image by

$$D = \frac{1}{MxN}\sum_{i=0}^{M-1}\sum_{j=0}^{N-1} f(i,j) \quad (5)$$

$\varphi(i,j)$ in Eq. (4) is the standard deviation value in the regional field *nxn* stated as

$$\varphi(i,j) = \sqrt{\frac{1}{nxn}\sum_{x=0}^{n-1}\sum_{y=0}^{n-1}(f(x,y) - m(i,j)^2} \quad (6)$$

The LTF in Eq. (2) is used for comparison with the proposed RSTF, where *a*, *b*, *c*, and *k* are parameters obtained by optimizing with DA.

2.2. Proposed Regional Similarity Transformation Function

The proposed function in this study is the Regional Similarity Transfer Function (RSTF) that performs a transformation on each pixel by considering the density distribution similarity between adjoining pixels.

$$g(i,j) = \frac{|k * f(i,j) - c * Max|}{\varphi(i,j) + b} + S(i,j)^a * f(i,j) \quad (7)$$

In Eq. (7), *S(i,j)* refers to the similarity value of the pixel at *(i,j)* with surrounding pixels, and is calculated through the following procedure of Eqs. (8) - (12). To determine the similarity value of the pixels in a 3x3 mask, the distances between pixels within the mask are required to build a relation matrix. Assuming two pixels, *k* and *l*, within the mask, the distance between the two, P_k and P_l, is determined [26].

$$d_{kl} = |P_k - P_l| \quad (8)$$

The exponential function in Eq. (9) is next used to calculate the similarity value of the two pixels resulting in a distribution range of similarity measurement varying from 0 to 1. If the value obtained from this function is near zero, then the two pixels are not similar. They are considered similar, if the value is near one [27].

$$S_{(k,l)} = exp^{(-\frac{d_{kl}}{D})} \tag{9}$$

In Eq. (9), D is the normalization coefficient and the results achieved can be graded by assigning 32, 64, 128, and 255 values. With nine pixels, the mask creates a 9x9 similarity relation matrix among adjacent pixels represented as

$$\begin{bmatrix} S(1.1) & \cdots & S(1.9) \\ \cdots & \cdots & \cdots \\ S(9.1) & \cdots & S(9.9) \end{bmatrix} \tag{10}$$

The arithmetic means of the relation matrix in Eq. (10) is calculated, and the similarity value to be included in the similarity image for the central pixel is calculated according to.

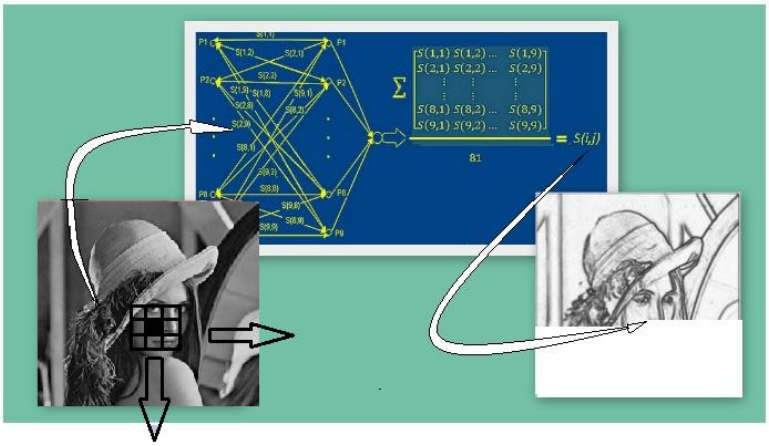
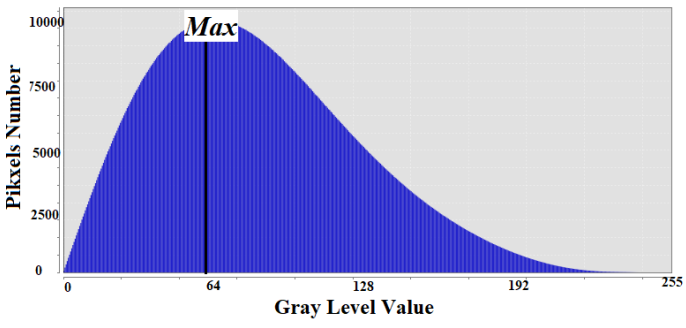


Figure 1. A symbolic representation of the presence of *S(i,j).*

$$S(i,j) = \frac{1}{81} * \sum_{k=1}^{9} \sum_{l=1}^{9} S_{kl} \tag{11}$$

The value obtained in Eq. (11) is assigned to the newly created similarity image by considering the address of the central pixel on the real image.




```
for from i=1 to number of row
    for from j=1 to number of columns
        v=Image(i,j);
        frequency(v+1)= frequency(v+1)+1;
    end for
end for

max_gray=max(frequency);

for from j=1 to number of columns
        if max_gray=frequency(k);
        Max=k;
        end if
end for
```

Figure 2. Pseudo code and symbolic representation of the *Max* value.

The mask panning is realized for the next operation, which is continued until the similarity value of the last pixel in the lower-right corner of the real image is found. A symbolic representation of the presence of *S(i,j)* is shown in Fig. 1.

In Eq. (7), *Max* provides the most used gray level value in the image. In the transformation function, if the distance of the pixel to *Max* is larger, then the spread and the value increase. The pseudo code and a symbolic demonstration of the calculation of *Max* are shown in Fig. 2.

In this study, DA optimizes the *a*, *b*, *c*, and *k* parameter values of Eq. (7), and the fitness function of the DA is evaluated below.

2.3. Evaluation Criteria

An objective evaluation criterion measures the quality of the images enhanced by the RSTF parameters by combining three performance measurements of entropy values, the total of edge intensities, and the number of edges in the image [14]. The objective stated in Eq. (12) foregrounds the edge count of edges and the high-density values of the edges [28].

$$F(x) = \frac{log\left(log\left(E\left(I(x)\right)\right)\right) * n_{edge}\left(I(x)\right) * H(I(x))}{M * N} \tag{12}$$

Here, $H(I(x))$ refers to entropy value of the image, $n\text{edge}(I(x))$ refers to the number of edge pixel in the image, and $E(I(x))$ refers to the sobel value of the image. M and N are the image dimensions.

2.4. Dragonfly Algorithm

A dragonfly is characterized by multifaceted eyes, two pairs of strong, transparent wings, and an elongated body. Unique and rare intelligent behaviors are observed through their hunting characteristics. In a static herd, they fly in small groups and move forward and backward while hunting. The key characteristics of a static dragonfly herd include local movements and sudden changes in the flight path.

According to the Reynold-inspired heuristic optimization techniques based on herds, herd behaviors features three principles [29]. Separation prevents clashing with adjoining individuals. Alignment refers to speed compliance with adjoining individuals. Cohesion represents the trend of the individuals towards the center of the adjoining mass. The primary goal of any herd is to survive, so individuals tend to move toward food sources. In addition, they can be interfered with from external predators. Combing these two behaviors, five factors are identified in a location update process as shown in Fig. 3. [30].

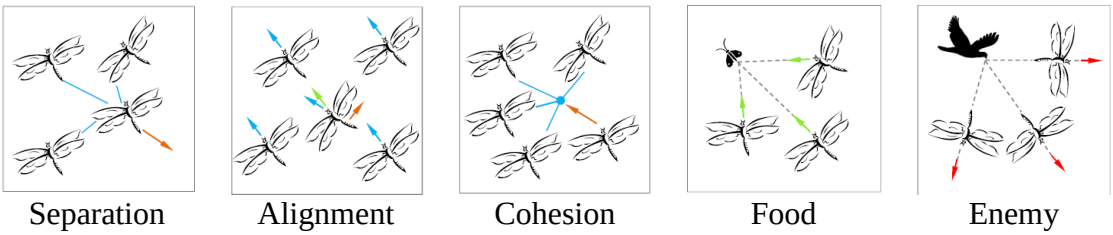


Figure 3. Primitive corrective patterns by individuals in a swarm [31].

Each behavior is modelled as the following.

$$S_i = -\sum_{j=1}^{N} X - X_j \tag{13}$$

In Eq. (13), X refers to position of the current individual and X_j shows the position of the j adjoining individual. N refers to number of adjoining individuals.

$$A_i = \frac{\sum_{j=1}^{N} V_j}{N} \tag{14}$$

In Eq. (14), V_j refers to the speed of the j adjoining individual. The cohesion is calculated as follows:

$$C_i = \frac{\sum_{j=1}^{N} X_j}{N} - X \tag{15}$$

$$F_i = X^+ - X \tag{16}$$

In Eq. (16), $X+$ is the position of the food source. In the event of an enemy threat, the outward behavior is by Eq. (17), where X^- is the position of the predator.

$$E_i = X^- + X \tag{17}$$

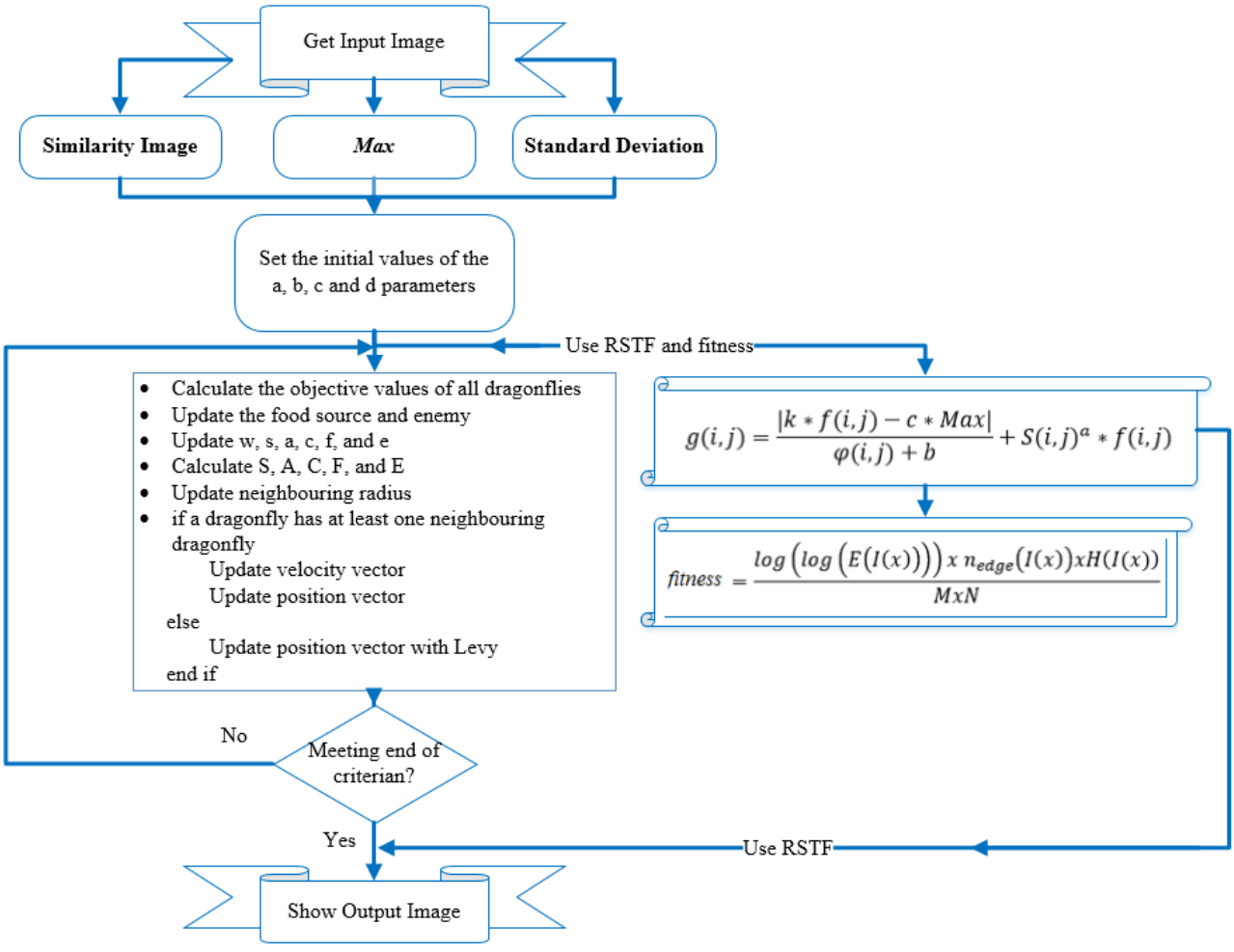


Figure 4. A flow chart for the Gray Image Enhancement Implementation Procedure Using RSTF and DA.

To update positions of artificial dragonflies in our algorithm by modelling these behaviors, two vectors, ΔX and X, are incorporated.

$$\Delta X_{t+1} = (sS_i + aA_i + cC_i + fF_i + eE_i) + w\Delta X_t \quad (18)$$

In Eq. (18), *s* refers to separation, *a* refers to alignment, *c* refers to cohesion, *f* refers to food, and *e* refers to a weight value from enemy factors. In addition, w is an inertial weight in the t iteration. After this step vector is calculated, the position vector is calculated as

$$X_{t+1} = X_t + \Delta X_{t+1} \quad (19)$$

A random walk (Le'vy flight) improves the properties of randomness, stochastic behavior, and artificial dragonfly discovery. In this case, positions of the dragonflies are updated using [30].

$$X_{t+1} = X_t + Le'vy(d) * X_t \quad (20)$$

In Eq. (20), *t* refers to the current iteration and *d* is the position vector.

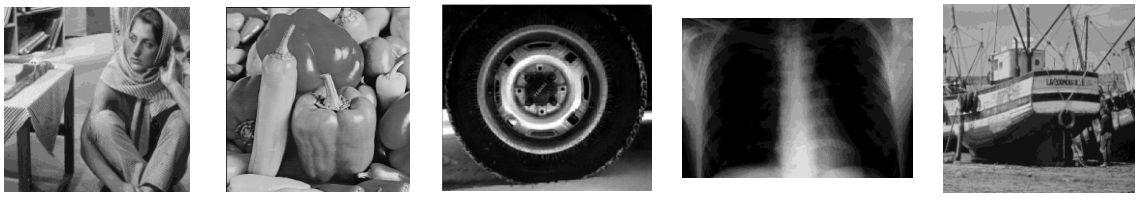
3. Gray Image Enhancement Implementation Procedure Using RSTF and DA

After the input image is captured, the Gray Image Enhancement Implementation Procedure Using RSTF and DA method for the similarity value in the 3x3 mask is found with Eq. (11). The Max values are determined with a standard deviation from Eq. (6) and the pseudo code from Fig. 2. As these values never change during the process, it is calculated before the search process. The agent and maximum iteration number of the DA optimization algorithm are entered. As shown in the flowchart in Fig. 4., the RSTF function results from Eq. (7) are found for the a, b, c, and k values formed randomly for each search agent. The image transfer function of Eq. (12) is inserted into the evaluation function and eligibility is evaluated.

After conformity assessment, speed and position updates from the DA are performed as shown in the rectangular profiles in Fig. 4. This section is repeated until the stopping criterion is provided. The best values of a, b, c, and k are obtained when the stopping criterion is met, and then inserted into the RSTF function of Eq. (7) to obtain the improved image.

4. Simulation Results and Analysis

The Barbara image is preferred to evaluate the performance of RSTF for different aspects as it offers a large size, average pixel intensity values, and narrow contrast. The Peppers image is in the same in jpg format, small, and has a wide contrast range. The Tire images used in this study are small with different row and columns as well as a small pixel density and contrast range. While the X-ray image has different row and column numbers and its pixel intensity variety is low in the png format, the Boat image offers a wider pixel intensity variety and is in a larger bmp format, as is often used in the literature. The images used in the proposed study are given in Fig. 5. and their technical characteristics are given in Table 1.



Barbara Peppers Tire X-ray image Boat

Figure 5. Images used in the study.

The range of the *a*, *b*, *c*, and *k* parameters in the RSTF are determined as $a \in [0,3]$, $b \in [0,0,5]$, $c \in [0,1]$, and $k \in [0,1]$. In the proposed method, the values for DA are maximum iteration = 15 and number of agents = 15. The algorithms were run with MATLAB R2012b using an Intel (R) Core (TM) i5-4200U CPU 2.30 GHz processor and 6 GB RAM.

Table 1. Objective evaluation results**.**

Name	Met.	Func.	Best	Mean	SD	Time	Parameters			
Barbara	PSO	LTF	0,8704	0,8686	0,0067	2,5192	1,2727	0,3960	0,9778	1,4500
		RSTF	0,9515	0,9484	0,0119	3,3737	1,2118	1,0900	0,6743	0,7974
	DE	LTF	1,1220	1,1030	0,0430	2,7582	0,9371	0,1340	0,8105	0,9061
		RSTF	1,1487	0,9097	0,0045	3,4938	2,0068	1,1316	0,5633	0,3520
	GSA	LTF	1,2180	1,2030	0,0180	1,9351	1,2273	0,0866	0,9670	0,7679
		RSTF	1,2224	1,2142	0,0066	3,2871	2,0895	1,5411	0,8937	0,4100
	DA	LTF	**1,2512**	**1,2316**	**0,0119**	**1,7981**	**1,1109**	**0,0785**	**0,9792**	**1,0418**
		RSTF	**1,2721**	**1,2253**	**0,0087**	**3,2465**	**2,0000**	**1,8166**	**1,0000**	**0,4659**
Peppers	PSO	LTF	0,8190	0,8144	0,0180	0,5270	1,4828	0,1337	0,9641	1,4361
		RSTF	0,8413	0,8413	0,0120	0,6651	2,1682	1,8953	0,8052	0,5000
	DE	LTF	0,7525	0,7120	0,0493	0,7021	1,2701	0,2569	0,6901	0,6582
		RSTF	0,7695	0,7495	0,0026	0,8918	2,1384	1,8341	0,7750	0,2884
	GSA	LTF	0,7664	0,7418	0,0257	0,5369	1,1589	0,1293	0,9367	0,8213
		RSTF	0,7739	0,7731	0,0021	0,9429	2,3357	1,2430	0,4656	0,2212
	DA	LTF	**0,8772**	**0,8075**	**0,0653**	**0,5176**	**0,6275**	**0,0306**	**1,0000**	**1,1000**
		RSTF	**0,9541**	**0,9502**	**0,0047**	**0,8856**	**2,5000**	**2,0000**	**0,6910**	**0,2704**
Tire	PSO	LTF	0,6355	0,6250	0,0085	0,5739	0,6176	0,1104	0,2355	0,8539
		RSTF	0,6993	0,6761	0,0095	0,6725	2,1780	1,1362	0,7156	0,5000
	DE	LTF	0,6921	0,6714	0,0208	0,9329	0,4743	0,2989	0,3351	1,4311
		RSTF	0,6997	0,6791	0,0056	1,2869	2,1019	1,1900	0,7861	0,1220
	GSA	LTF	0,6792	0,6723	0,0088	0,5690	0,5276	0,1004	0,4555	0,9254
		RSTF	0,6797	0,6792	0,0084	0,9685	2,0548	1,1941	0,6738	0,0654
	DA	LTF	**0,6985**	**0,6360**	**0,0359**	**0,5312**	**0,7050**	**0,0271**	**0,8602**	**0,8789**
		RSTF	**0,6996**	**0,6788**	**0,0090**	**0,9713**	**2,2348**	**1,4842**	**0,8583**	**0,2643**
X-ray	PSO	LTF	0,7452	0,7023	0,0078	2,2145	0,7589	0,1256	0,9058	0,8263
		RSTF	0,7584	0,6962	0,0087	3,2655	2,8754	0,2056	0,8766	1,1170
	DE	LTF	0,7675	0,7115	0,0892	2,6552	0,5050	0,3284	0,8059	0,7813
		RSTF	0,7863	0,7245	0,0077	4,1630	2,2741	0,2367	0,6552	0,9363
	GSA	LTF	0,6852	0,6262	0,0625	1,9056	0,4978	0,0570	0,9317	1,4018
		RSTF	0,7145	0,6925	0,0143	3,2955	2,5517	0,1180	0,3412	0,8094
	DA	LTF	**0,7739**	**0,6640**	**0,1341**	**1,8168**	**0,7762**	**0,0250**	**1,0000**	**1,3032**
		RSTF	**0,8657**	**0,8610**	**0,0199**	**2,3351**	**3,0000**	**0,1302**	**0,6167**	**1,0000**
Boats	PSO	LTF	0,8739	0,8724	0,0058	1,3543	1,4586	0,1705	0,7622	0,8400
		RSTF	0,7977	0,7759	0,0672	1,6456	0,3414	0,8051	0,5147	0,5211
	DE	LTF	0,9491	0,9151	0,0291	1,7613	1,3365	0,4818	0,4132	1,0858
		RSTF	0,8410	0,7812	0,0687	2,2010	2,5121	0,2152	1,0041	0,7543
	GSA	LTF	1,0067	0,9847	0,0162	1,1756	0,9876	0,0494	0,9458	0,9155
		RSTF	1.0872	1,0092	0,1814	1,5537	2,2781	0,1876	0,4597	0,1858
	DA	LTF	**1,0196**	**0,9460**	**0,0548**	**1,1949**	**0,8300**	**0,0356**	**1,0000**	**1,0000**
		RSTF	**1,1117**	**1,0790**	**0,1619**	**1,5511**	**2,8862**	**0,3000**	**1,0000**	**0,5185**

4.1 Comparing the Results of RSTF and DA

The RSTF proposed above and the LTF from the literature are compared in terms of optimization searching results. The evaluation criteria of the RSTF and LTF transformation functions consist of total entropy values, number of edge pixels, and pixel intensity of the images. The transformation

functions parameters are optimized using DA [31]. Also, to test the performance of the DA, Particle Swarm Optimization (PSO), Differential Evolution (DE) and Gravitational Search Algorithm (GSA) heuristic optimization techniques are applied [31, 32, 33].

The averages of the best, mean, standard deviation (SD), and time are calculated by running these four heuristic optimization techniques 30 times on each image. The parameter coefficients for the final run is added to Table 1. As shown in these results, DA provides better results for all five images compared to the other three optimization techniques. The best and mean values are larger than those from GSA, PSO, and DE. The DA results clearly demonstrates it found the best results as well as performed the search quickest.

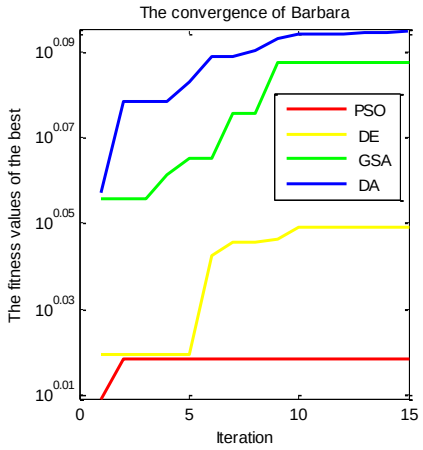


Figure 6. Barbara convergence graphs using PSO, DE, GSA, and DA techniques for RSTF.

Table 2. The suitability values for Barbara RSTF.

	Entropy	Edge Pixels	Edge Intensity
PSO	7,5259	14579	$1.291.10^5$
DE	7,6638	15361	$1.044.10^5$
GSA	7,8171	16625	$1.336.10^5$
DA	7,8171	16625	$1.336.10^5$

When RSTF and LTF in Table 1 are compared, the best and mean results of RSTF are satisfactory. The high compliance values show that the RSTF transformation function performs with the correct parameters. The similarities in Eq. (11) and the histogram over the *Max* calculation processes extend the time of RSTF.

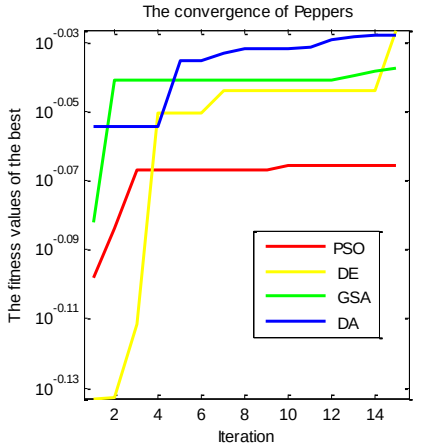


Figure 7. Peppers convergence graphs using PSO, DA, GSA, and DA techniques for RSTF.

Therefore, RSTF requires 25% longer operation time compared to LTF. As RSTF and LTF are different in terms of structure and parameter limits, a relationship or similarity must not be considered with the *a*, *b*, *c*, and *k* values.

According to the results of the evaluation criteria in Tables 2 - 4, when heuristic algorithms are compared for different control parameters, the highest success is achieved with DA. The convergence diagram comparison of the algorithms for the control parameters with the highest success achieved from the table is shown in Figs. 6 - 8. DA shows an efficient convergence in the PSO, DE, and GSA convergence diagrams for the Barbara, Peppers, and Tire images.

Table 3. The suitability values for Peppers RSTF.

	Entropy	**Edge Pixels**	**Edge Intensity**
PSO	7,5513	14913	$9.673.10^4$
DE	7,6638	15361	$1.044.10^5$
GSA	7,6701	15604	$1.954.10^5$
DA	7,7742	16214	$2.385.10^5$

4.2 Image Quality Assessment for RSTF

Measuring image quality is important for most image processing applications. In this section, performance is inspected using objective evaluation methods of the output image obtained with the RSTF. The first method of the Mean Square Error (MSE) defines the similarity or distortion level between the output and input images.

$$MSE = \frac{1}{MN}\sum_{n=1}^{M}\sum_{m=1}^{N}[I(x,y) - I'(x,y)]^2 \tag{21}$$

In Eq. (21), *I(x,y)* refers to the input image, *I'(x,y)* refers to the output image, and *M* and *N* refer to the row and column number of the image. An MSE value close to zero shows similarity between the output and input images. Therefore, finding small values in MSE shows the difficulty of the proposed method [34].

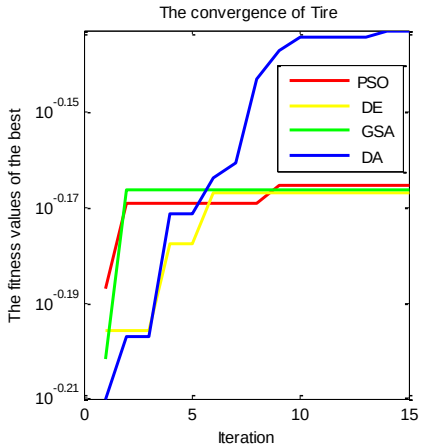


Figure 8. Tire convergence graphs using PSO, DE, GSA, and DA techniques for RSTF.

The alternate method of Peak to Signal Noise Ratio (PSNR) is a measure of the top error and is used in success analysis as an error criterion. When the PSNR value is high, the output image quality obtained with the proposed conversion function increases [35].

Table 4. The suitability values for Tire RSTF

	Entropy	Edge Pixels	Edge Intensity
PSO	7,0075	2776	$3.134.10^4$
DE	7,0546	2823	$3.419.10^4$
GSA	6,9158	2989	$4.311.10^4$
DA	7,2729	3166	$4.745.10^4$

PSNR has a logarithmic scale and is calculated by Eq. (22) where L refers to the maximum pixel intensity value of the input image.

$$PSNR = 10\log_{10}\frac{L^2}{MSE} \tag{22}$$

Normalized Cross Correlation (NCC) is another common comparison criterion is obtained by coinciding the input and output images. The correlation coefficient, r, defined in Eq. (23) is considered as the best coincidence when it has the highest value [36].

$$r = \frac{\sum_{n=1}^{M}\sum_{m=1}^{N} I(x,y)I'(x,y)}{\sqrt{\sum_{n=1}^{M}\sum_{m=1}^{N} I(x,y)^2 \sum_{n=1}^{M}\sum_{m=1}^{N} I'(x,y)^2}} \tag{23}$$

Structural Content (SC) concerns spacial regulations of pixels in the image and can reveal a close relation between input and output images. A high value of SC indicates the quality of the output image is poor.

$$SC = \frac{\sum_{i=1}^{M}\sum_{j=1}^{N} I(i,j)^2}{\sum_{i=1}^{M}\sum_{j=1}^{N} I'(i,j)^2} \tag{24}$$

The Average Difference (AD) is directly proportional with the contrast and shows two dynamic ranges of the image. A high value of AD shows that the output image is poor [37].

$$AD = \frac{1}{MN}\sum_{i=1}^{M}\sum_{j=1}^{N}(I(i,j) - I'(i,j)) \tag{25}$$

Structural Similarity Index Measurement (SSIM) consists of three terms and is an effective way to predict the visual impact of the image brightness, contrast, and structural changes. In Eq. (26), *l(x, y)* refers to brightness, *c(x, y)* refers to contrast, and *s(x, y)* are the components that represent the structural changes [38].

$$SSIM = [l(x,y)]^{\alpha}[c(x,y)]^{\beta}[s(x,y)]^{\gamma} \tag{26}$$

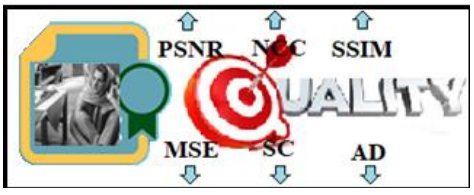


Figure 9. Expected results from the objective assessment methods for Image Quality Assessment.

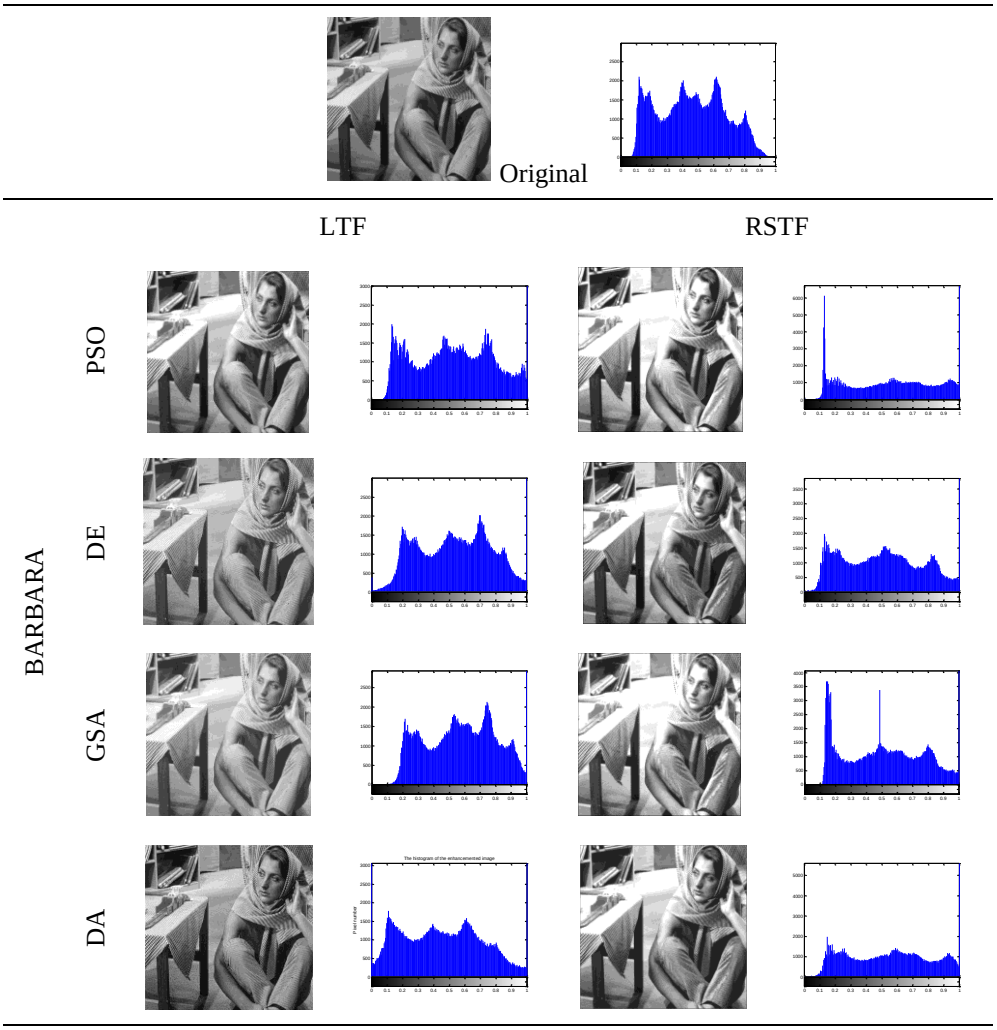


Figure 10. RSTF and LTF visual results for Barbara.

Table 5. RSTF and LTF image quality visual results for Barbara.

Name	Met.	Fun.	MSE	PSNR	NCC	SC	AD	SSIM
Barbara	PSO	LTF	$1.643.10^4$	5,973	0,0035	$7.903.10^4$	117,000	0,0043
		RSTF	$1.629.10^4$	5,981	0,0052	$3.612.10^4$	116,795	0,0065
	DE	LTF	$1.657.10^4$	5,937	0,0058	$2.915.10^4$	116,936	0,0077
		RSTF	$1.650.10^4$	5,939	0,0059	$2.938.10^4$	116,823	0,0078
	GSA	LTF	$1.663.\ 10^4$	5,960	0.0039	$6.334.10^4$	116.869	0.0079
		RSTF	$1.669.10^4$	5,982	0,0059	$3.533.10^4$	116,782	0,0079
	DA	LTF	$1.662.\ 10^4$	5,923	0.0043	$5.333.10^4$	116.902	0.0056
		RSTF	**$1.619.10^4$**	**5,990**	**0,0059**	**$2.873.10^4$**	**116,913**	**0,0083**

As a result of transformation function, excessive brightness, blur, and deterioration in the images are resolved with the proposed method. Moreover, natural and wide contrast enhancement is also obtained on the images according to the values in Table 5 for the Barbara image. Especially high values from the PSNR, NCC, and SSIM calculations show the quality of output image.

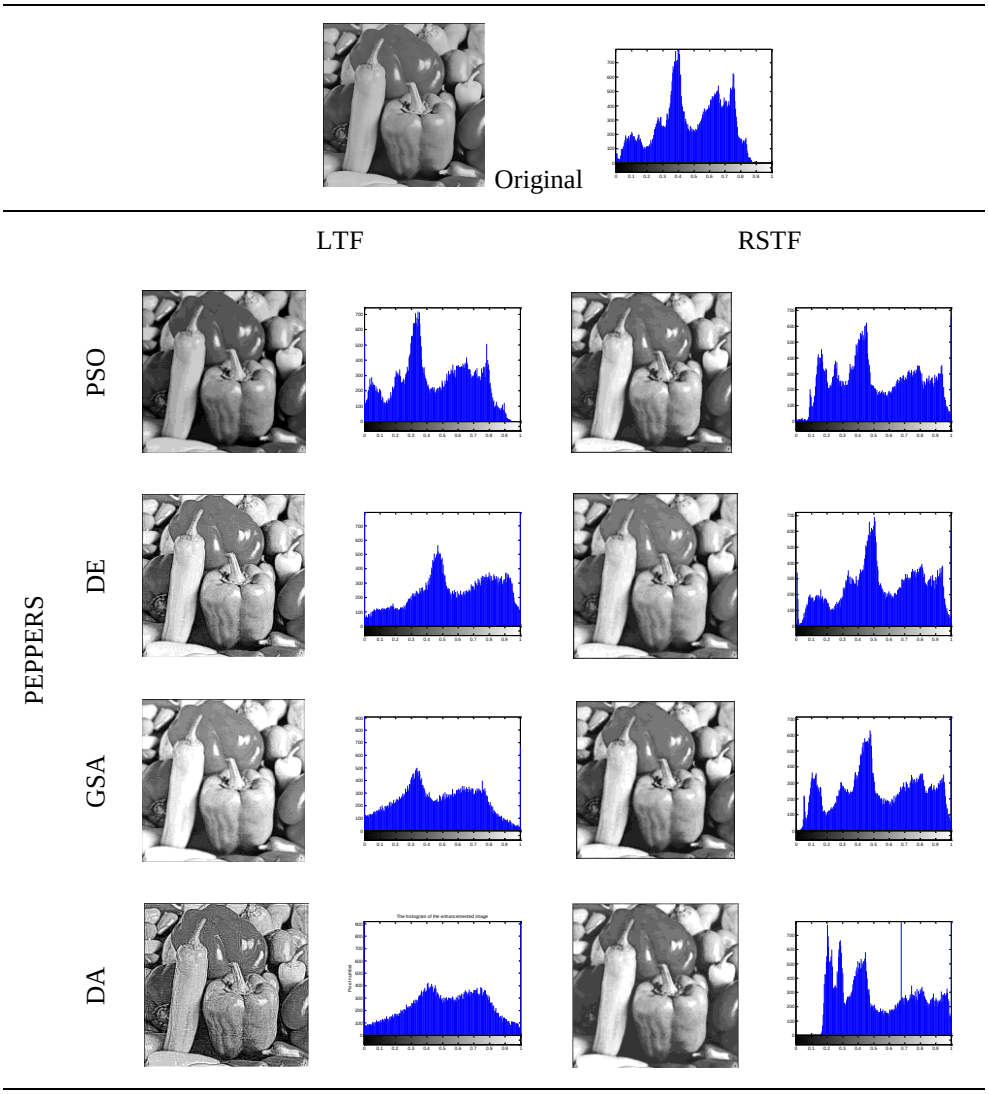


Figure 11. RSTF and LTF visual results for Peppers.

The same enhancements and results as seen in the Barbara image are also found in the Peppers image. Since the Peppers image is small with a wide contrast range, visual enhancement is less. Examining Fig. 11., the difference between LTF and RSTF is seen in the histogram curves. For RSTF, the pixel number in the areas increased to nearly 255 without distorting the histogram curve. The middle gray level reproduction is seen in LTF, which is an important small change seen in Table 6.

Table 6. RSTF and LTF image quality visual results for Peppers.

Name	Met.	Fun.	MSE	PSNR	NCC	SC	AD	SSIM
Peppers	PSO	LTF	$1.784.10^4$	5,615	0,0037	$7.096.10^4$	122,677	0,0052
		RSTF	$1.781.10^4$	5,622	0,0044	$5.004.10^4$	122,562	0,0070
	DE	LTF	$1.780.10^4$	5,625	0,0047	$4.409.10^4$	122,527	0,0070
		RSTF	$1.780.10^4$	5,624	0,0047	$4.356.10^4$	122,518	0,0072
	GSA	LTF	$1.782.10^4$	5,620	0,0043	$4.480.10^4$	122,586	0,0064
		RSTF	$1.780.10^4$	5,627	0,0048	$4.006.10^4$	122,562	0,0070
	DA	LTF	$1.782.10^4$	5,620	0,0042	$5.210.10^4$	122,591	0,0064
		RSTF	**$1.780.10^4$**	**5,629**	**0,0048**	**$4.960.10^4$**	**122,515**	**0,0072**

The process of improving images with narrow contrast regions, such as the Tire image in Fig. 12., where the color pixel density variability is minimal, can result in excessive brightness or dark areas in the image. The contrast setting of RSTF increases or decrease according to the similarity value of adjoining pixels. Since the similarity values are very close in single type gray level valued images, such as the Tire image, the contrast in the image is visibly changed. However, as in LTF, excessive brightness results and visual loss is prevented. Likewise, as seen in Fig. 12., the brightness is achieved in small increments due to the proximity to the *Max* value for all pixels. Table 7 shows the results of the comparison between the input and output images as a result of applying the LTF and RSTF to the Tire image. The comparison is close with a slight favor for RSTF. However, in general, the RSTF cannot make the desired enhancements in uniform images with varying pixel values.

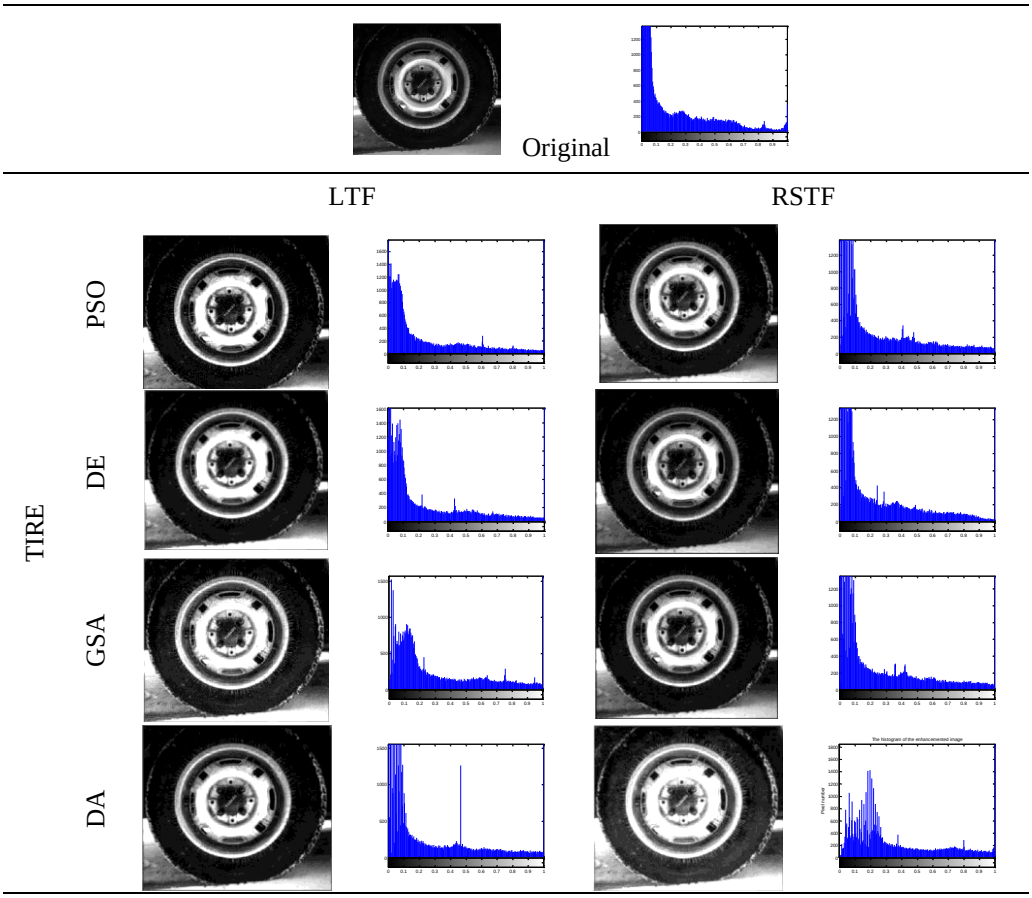


Figure 12. RSTF and LTF visual results for Tire.

Table 7. RSTF and LTF image quality visual results for Tire.

Name	Met.	Fun.	MSE	PSNR	NCC	SC	AD	SSIM
Tire	PSO	LTF	$6.984.10^3$	9,720	0,0061	$1.439.10^4$	54,319	0,1009
		RSTF	$6.973.10^3$	9,792	0,0081	$1.370.10^4$	54,240	0,1077
	DE	LTF	$6.943.10^3$	9,715	0,0075	$1.659.10^4$	54,013	0,1241
		RSTF	$6.921.10^3$	9,728	0,0075	1.498.104	54,002	0,1280
	GSA	LTF	$6.924.10^3$	9,726	0,0081	$1.223.10^4$	53,595	0,1188
		RSTF	$6.915.10^3$	9,690	0,0088	$1.214.10^4$	53,258	0,1206
	DA	LTF	$6.942.10^3$	9,715	0,0075	$1.676.10^4$	54,051	0,1187
		RSTF	**$6.905.10^3$**	**9,798**	**0,0088**	**$1.160.10^4$**	**53,220**	**0,1281**

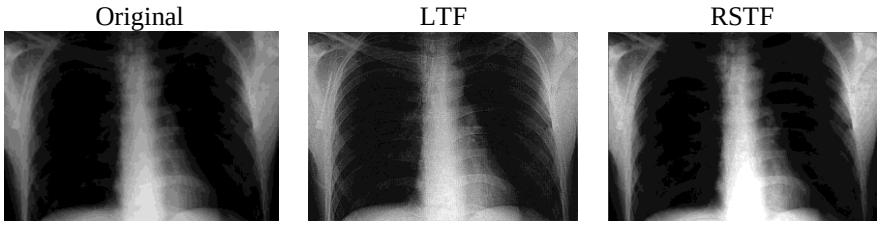


Figure 13. Image comparisons with DA for the *X*-ray image.

Table 8. Comparison of suitability values with DA for the X-ray image.

DA		Entropy	Edge Pixels	Edge Intensity
	Original	5,8561	6681	$1.7622.10^4$
	LTF	7,5597	10533	$6.8657.10^4$
	RSTF	7,9817	10787	$7.6227.10^4$

Tables 8, Fig. 13 with the X-ray and Table 9, Fig. 14 with Boats images also show the DA and RSTF performance as tested with the entropy, edge pixel, and edge intensity properties. These three comparison values obtained from the RSTF image are more satisfactory than those from the original and LTF images. The visual results of the proposed RSTF method are alsobetter than the LTF images. Detailed sections are clearly visible in the dark region, and the foreground, background, and the target can be clearly distinguished as the noise is effectively rejected in the images.



Figure 14. Image comparisons with DA for the Boats image.

Table 9. Comparison of suitability values with DA for the Boats image.

DA		Entropy	Edge Pixels	Edge Intensity
	Original	7,2171	7520	$4.5588.10^4$
	LTF	7,8098	8644	$1.1870.10^5$
	RSTF	7,9240	8855	$1.2077.10^5$

5. Conclusions

In this study, a regional similarity transformation function is proposed as a new method for image enhancement. By optimizing the parameters of the transformation function, the success of this method is increased. The results of the proposed method RSTF are applied to the LTF conversion function with PSO, DE, and GSA optimization techniques and compared with the use of DA. In the LTF method, there is excessive brightness or low contrast on the images without effective enhancement for all images. The heuristic algorithms implemented with RSTF also provide effective enhancements in images in terms of visual and information quality. The proposed DA-

based RSTF method provides an effective enhancement by adjusting the natural contrast and brightness on the images.

The basic structure, speed, and real value convergence features should be used in optimization-based applications of image processing. The resulting Gray Image Enhancement Using RSTF and DA is preferred overall image processing applications because it performs faster while being more powerful and convenient to use. Therefore, in the next study, the RSTF method applied to infrared and color images is considered for enhancement processing.

Acknowledgments

The author declare that He did not receive any funding for this study. Also, the authors declare that they have no conflict of interest.

References

[1]. Schalkoff, R. J., Digital image processing and computer vision, New York: Wiley Vol. 286 (1989).
[2]. Gonzalez, R. C.; Woods, R. E., Digital image processing. (2012).
[3]. Russ, J. C., The image processing handbook, CRC press. (2016) .
[4]. Kim, Y. T., Contrast enhancement using brightness preserving bi-histogram equalization, IEEE transactions on Consumer Electronics, 1997, 43(1): 1-8.
[5]. Wang, Q.; Ward, R. K., Fast image/video contrast enhancement based on weighted thresholded histogram equalization, IEEE transactions on Consumer Electronics, 2007, 53(2)
[6]. Chen, S. D.; Ramli, A. R., Contrast enhancement using recursive mean-separate histogram equalization for scalable brightness preservation, IEEE Transactions on consumer Electronics, 2003, 49(4): 1301-1309.
[7]. Sim, K. S.; Tso, C. P.; Tan, Y. Y., Recursive sub-image histogram equalization applied to gray scale images, Pattern Recognition Letters, 2007, 28(10): 1209-1221.
[8]. Tanaka, G.; Suetake, N.; Uchino, E., Image enhancement based on multiple parametric sigmoid functions, In Intelligent Signal Processing and Communication Systems, ISPACS 2007 IEEE, 2007, 108-111.
[9]. Kannan, P.; Deepa, S.; Ramakrishnan, R., Contrast enhancement of sports images using modified sigmoid mapping function, In Communication Control and Computing Technologies (ICCCCT), 2010 IEEE International Conference, 2010, 651-656.
[10]. Verma, H. K.; Pal, S., Modified Sigmoid Function Based Gray Scale Image Contrast Enhancement Using Particle Swarm Optimization, Journal of The Institution of Engineers (India): Series B, 2016, 97(2): 243-251.
[11]. Munteanu, C.; Lazarescu, V., Evolutionary contrast stretching and detail enhancement of satellite images, Proceedings of MENDEL'99, 1999, 94-99.
[12]. Saitoh, F., Image contrast enhancement using genetic algorithm, In Systems, Man, and Cybernetics, 1999. IEEE SMC'99 Conference Proceedings. 1999 IEEE International Conference, 1999, 4: 899-904.
[13]. Munteanu, C.; Rosa, A., Towards automatic image enhancement using genetic algorithms, In Evolutionary Computation, 2000. Proceedings of the 2000 Congress, 2000, 2: 1535-1542.
[14]. Gorai, A.; Ghosh, A., Gray-level image enhancement by particle swarm optimization, In Nature & Biologically Inspired Computing, NaBIC, 2009, 72-77.
[15]. Zhao, W., Adaptive image enhancement based on gravitational search algorithm, Procedia Engineering, 2011, 15: 3288-3292.

[16]. Agrawal, S.; Panda, R., An efficient algorithm for gray level image enhancement using cuckoo search, In International Conference on Swarm, Evolutionary, and Memetic Computing, Springer, Berlin, Heidelberg, 2012, 82-89.
[17]. Sarangi, P. P.; Mishra, B. S. P.; Majhi, B.; Dehuri, S., Gray-level image enhancement using differential evolution optimization algorithm, In Signal Processing and Integrated Networks (SPIN), 2014, 95-100.
[18]. Murali, K.; Jayabarathi, T., Automated image enhancement using Grey-wolf optimizer algorithm, J Multidiscip Sci Technol, 2016, 7: 77-84.
[19]. Draa, A.; Bouaziz, A., An artificial bee colony algorithm for image contrast enhancement, Swarm and Evolutionary computation, 2014, 16: 69-84.
[20]. Demircioğlu, P., Diş ve İmplant Mikromorfolojik Yapıların Sinyal ve Görüntü İşleme Yöntemleri ile Değerlendirilmesi, El-Cezeri Journal of Science and Engineering, 2018, 5(3): 741-748.
[21]. Güvenoğlu, E.; Razbonyalı, C., The Creation of Maze in Order to Hide Data, and the Proposal of Method Based on AES Data Encryption Algorithm, El-Cezeri Journal of Science and Engineering, 2019, 6(3): 668-680.
[22]. Katırcıoğlu, F., Real-time infrared image processing for control and monitoring of greenhouse system, Journal of Applied Remote Sensing, 2020, 14(2): 026503.
[23]. Enginoğlu, S.; Erkan, U.; Memiş, S., Adaptive Cesáro Mean Filter for Salt-and-Pepper Noise Removal. El-Cezeri Journal of Science and Engineering, 2019, 7(1): 304-314.
[24]. Katırcıoğlu, F.; Çay, Y.; Cingiz, Z., Infrared image enhancement model based on gravitational force and lateral inhibition networks, Infrared Physics & Technology, 2019, 100: 15-27.
[25]. Ozturk, S.; Ozturk, N., Yapay arı koloni algoritması kullanarak görüntü iyileştirme yönteminin geliştirilmesi, Gazi University Fen Bilimleri Dergisi Part C: Tasarım ve Teknoloji, 2016, 4(4): 173-183.
[26]. Demirci, R.; Katircioglu, F., Segmentation of color images based on relation matrix, Signal Processing and Communications Applications, SIU 2007, 2007.
[27]. Katircioglu, F., Segmentation of color images based on relation matrix and edge detection, Master of Science, Dept. Electrical Education, Duzce Universtiy, Duzce, Turkey, 2007.
[28]. Ye, Z.; Wang, M.; Hu, Z.; Liu, W., An adaptive image enhancement technique by combining cuckoo search and particle swarm optimization algorithm, Computational intelligence and neuroscience, 2015, 13.
[29]. Reynolds, C. W., Flocks, herds and schools: A distributed behavioral model, In ACM Siggraph computer graphics, 1987, 21(4): 25-34.
[30]. Mirjalili, S., Dragonfly algorithm: a new meta-heuristic optimization technique for solving single-objective, discrete, and multi-objective problems, Neural Computing and Applications, 2016, 27(4): 1053-1073.
[31]. Kwok, N. M.; Ha, Q. P.; Liu, D.; Fang, G., Contrast enhancement and intensity preservation for gray-level images using multiobjective particle swarm optimization, IEEE Transactions on Automation Science and Engineering, 2009, 6(1): 145-155.
[32]. Dos Santos Coelho, L.; Sauer, J. G.; Rudek, M., Differential evolution optimization combined with chaotic sequences for image contrast enhancement, Chaos, Solitons & Fractals, 2009, 42(1): 522-529.
[33]. Rashedi, E.; Nezamabadi-Pour, H.; Saryazdi, S., GSA: a gravitational search algorithm, Information sciences, 2009, 179(13): 2232-2248.
[34]. Lee, J. S., Digital image enhancement and noise filtering by use of local statistics, IEEE transactions on pattern analysis and machine intelligence, 1980, 2: 165-168.

[35]. Prashanth, H. S.; Shashidhara, H. L.; KN, B. M., Image scaling comparison using universal image quality index, In Advances in Computing, Control, & Telecommunication Technologies, ACT'09, 2009, 859-86.
[36]. Nakhmani, A.; Tannenbaum, A., A new distance measure based on generalized image normalized cross-correlation for robust video tracking and image recognition, Pattern recognition letters, 2013, 34(3): 315-321.
[37]. Rajkumar, S.; Malathi, G. A comparative analysis on image quality assessment for real time satellite images, Indian Journal of Science and Technology, 2016, 9(34).
[38]. Wang, Z.; Bovik, A. C.; Sheikh, H.R.; Simoncelli, E. P., Image quality assessment: from error visibility to structural similarity, IEEE transactions on image processing, 2004, 13(4): 600-612.